Geosfera Indonesia
p-ISSN 2598-9723, e-ISSN 2614-8528
available online at : https://jurnal.unej.ac.id/index.php/GEOSI
Vol. 8 No. 2, August 2023, 189-205

https://doi.org/10.19184/geosi.v8i2.41214

Research Article

Mapping Seagrass Biodiversity Indicators of Pari Island using Multiple WorldView-2 Bands Derivatives

Pramaditya Wicaksono[1]*, Setiawan Djodi Harahap[2]
[1]Department of Geographic Information Science, Faculty of Geography, Universitas Gadjah Mada, DIY, 55281, Indonesia
[2]Master of Remote Sensing, Faculty of Geography, Universitas Gadjah Mada, DIY, 55281, Indonesia
*Corresponding Author, Email address: prama.wicaksono@ugm.ac.id

ARTICLE INFO

Received :
7 July 2023

Revised :
20 August 2023

Accepted :
25 August 2023

Published :
29 August 2023

ABSTRACT

Comprehensive information on seagrass biodiversity indicators, such as species composition, percentage cover, and biomass carbon stock, remains limited across various regions globally. Mapping these indicators using remote sensing images requires extracting maximum information from the input images to achieve effective results. This study aims to map seagrass distribution, percent cover (PC), and aboveground carbon stock (AGC) as biodiversity indicators in the optically shallow waters surrounding Pari Island. We integrate WorldView-2 (WV2) derivatives, field seagrass data, and RF classification and regression algorithms to accomplish this objective. The WV2 image derivatives encompass surface reflectance bands, band ratios, mean and variance co-occurrence texture bands, and principle component bands. These inputs are used individually and collectively for mapping, employing a random forest algorithm trained with field seagrass data. Our results demonstrate that the most accurate benthic habitat map achieves an overall accuracy (OA) of 65.2%, with a user's accuracy of 65.2% and a producer's accuracy of 72.8% for the seagrass-dominated class. Seagrass PC mapping yields a root mean square error (RMSE) of 17.1%, with an average PC of 47.4 ± 9.9%. Seagrass AGC mapping achieves an RMSE of 5.0 g C m-2, with an average AGC range of 6.2 – 29.1 g C m-2, estimating the study area's aboveground biomass carbon stock at 27.9 tons C. Combined inputs produce the most accurate results for all biodiversity indicators, emphasizing the importance of utilizing combined bands from SR band derivatives to maximize information input for training mapping algorithms, instead of using derivative bands individually or as replacements for the initial SR bands.

Keywords : Seagrass; Biodiversity; Mapping; WorldView-2; Pari Island

INTRODUCTION

Seagrass beds play a vital role in providing a wide range of ecosystem services, both ecologically and economically, at local and global levels (Nordlund et al., 2016; UNEP, 2020). They support a diverse array of marine biota, including fish, crustaceans, and sponges, which are essential for ensuring food security from the marine sector. Moreover, seagrass beds contribute to the prevention of coastal erosion, sediment stabilization, water purification, bacteria filtration, and serve as a rich source of biodiversity for marine animals. Additionally, they effectively absorb

carbon, making them a crucial component in efforts to adapt to and mitigate climate change (Fourqurean et al., 2012; Nordlund et al., 2016; UNEP, 2020). Therefore, the preservation of a healthy seagrass ecosystem is of utmost importance for climate change adaptation and mitigation, and a comprehensive understanding of seagrass ecosystem biodiversity is essential for effective ecosystem management and the maintenance of associated services.

Managing seagrass ecosystems requires a comprehensive understanding of the spatial and temporal distribution of their biodiversity. Mapping seagrass beds is best achieved through remote sensing, as demonstrated by numerous studies (Green et al., 2000; Hossain et al., 2015; Pittman et al., 2021). Remote sensing techniques have proven successful in mapping various indicators of seagrass biodiversity, including species composition, percentage cover, leaf area index (LAI), and aboveground biomass carbon stock (AGC) (Phinn et al., 2008; Wicaksono & Hafizt, 2013; Roelfsema et al., 2014; Wicaksono et al., 2019; Pittman et al., 2021; Wicaksono et al., 2022a; Wicaksono et al., 2022b; Wicaksono et al., 2022c).

To map seagrass, researchers have employed a range of inputs, starting from reflectance bands, sunglint-corrected bands, water column-corrected bands, texture bands, principle component bands, to band ratios (Wicaksono, 2016; Wicaksono et al., 2022a; Wicaksono et al., 2022b; Wicaksono et al., 2022c). Additionally, various types of remote sensing imagery, such as Landsat, Sentinel-2, IKONOS, Quickbird, PlanetScope, and WorldView-2, have been utilized (Hochberg, et al., 2003; Mishra, et al., 2006; Wicaksono, et al., 2019; Wicaksono et al., 2022a; Wicaksono et al., 2022b; Wicaksono et al., 2022c). Methodologies employed include parametric classification and regression, as well as non-parametric machine learning classification and regression (Pittman et al., 2021).

However, despite these advancement of remote sensing for seagrass mapping, comprehensive information regarding biodiversity indicators such as species composition, percentage cover, and biomass carbon stock remains limited across many regions of the globe. This scarcity is particularly evident when it comes to their spatial and temporal distribution. Previous studies have acknowledged the difficulties associated with mapping seagrass biodiversity using remote sensing techniques (Hossain et al., 2015; Wicaksono et al., 2019; Pittman et al., 2021). Consequently, to effectively map seagrass using remote sensing images, it is crucial to extract as much information as possible from the images used as the foundation for mapping. Fortunately, the advancement of machine learning approaches provides a viable solution for leveraging abundance information to map seagrass. Hence, in this study, we employed various image analysis techniques to derive various unique information from the WorldView-2 bands, which can be used in conjunction with the original reflectance bands of WorldView-2, to map seagrass biodiversity indicators.

The objective of this research is to utilize the integration of WorldView-2 derivatives, field seagrass data, and machine learning classification and regression algorithms to map seagrass biodiversity indicators in a specific area of Pari Island. The mapped indicators of biodiversity in this study encompass seagrass distribution, percent cover, and above-ground carbon stock (AGC). WorldView-2 (WV2) imagery was selected due to its ability to detect underwater objects using its six visible bands. Although WorldView-3 (WV3) imagery has similar underwater object detection capabilities and offers a higher spatial resolution compared to WV2, it is regrettably unavailable on Pari Island. Alternatively, Planet SuperDove imagery features a high spectral resolution with seven bands that could potentially detect underwater objects. However, the effective utilization of SuperDove imagery for mapping underwater objects is hindered by significant noise and inconsistent radiometric image quality, particularly in water areas (Wicaksono et al., 2022b).

STUDY AREA

The study area chosen for this research manuscript is Pari Island, located in the Thousand Islands area of DKI Jakarta Province. This region has limited spatially- and temporally-extensive information regarding seagrass biodiversity. Pari Island, known for its rich seagrass biodiversity,

possesses distinct characteristics in its seagrass beds, such as variations in substrate, species diversity, water clarity, depth, and epiphytic cover. Due to its popularity as a tourist destination for individuals from the Greater Jakarta area, Pari Island experiences significant human activity, particularly along its coastline where seagrass beds are directly affected.

Pari Island harbors seagrass beds dominated by Enhalus acoroides (Ea) and Thalassia hemprichii (Th), along with other species including Syringodium isoetifoleum (Si), Cymodocea rotundata (Cr), Halodule uninervis (Hu), and Halophila ovalis (Ho). Seagrass beds can be categorized into two types based on their location. The first type is found on the south, northeast, and southeastern sides of Pari Island, situated on reef flats with clear, shallow water, white carbonate sand substrates, low epiphytic cover, and a dominance of Th and Cr species. The second type is found on reef flats and lagoons, characterized by turbid water conditions, a mixed substrate of sand and silt, high epiphytic cover, and a prevalence of Ea species with long leaves and high density. The elongated leaves of Ea may be an adaptation to maximize light absorption for photosynthesis in turbid waters. This characteristic is observed from the northwest side of the island to the deep lagoon. The tide on Pari Island follows a diurnal pattern (single daily tide) (Widisanto et al., 2022). Considering these conditions, it can be deduced that the biodiversity of seagrass beds on Pari Island is influenced by substrate conditions, water quality, water depth, tides, and epiphytic cover.

Pari Island, as a popular tourist destination, attracts an annual average of 60,000 visitors (BPS Kepulauan Seribu, 2022). However, the island's waste management system is facing increasing pressure due to community activities, resulting in a growing waste problem. Unfortunately, much of this waste ends up buried in the roots of mangroves and the canopies of seagrass (based on direct field observation). Therefore, there is an urgent need for up-to-date spatial and temporal information on seagrass beds. This information plays a crucial role in monitoring the impact of community activities and ensuring the effectiveness of waste management practices. The study was conducted on Pari Island, located in Kepulauan Seribu, DKI Jakarta, as shown in Figure 1. The specific focus area for this study, indicated by the red polygon in the figure, was determined based on the availability of the latest WorldView-2 images.

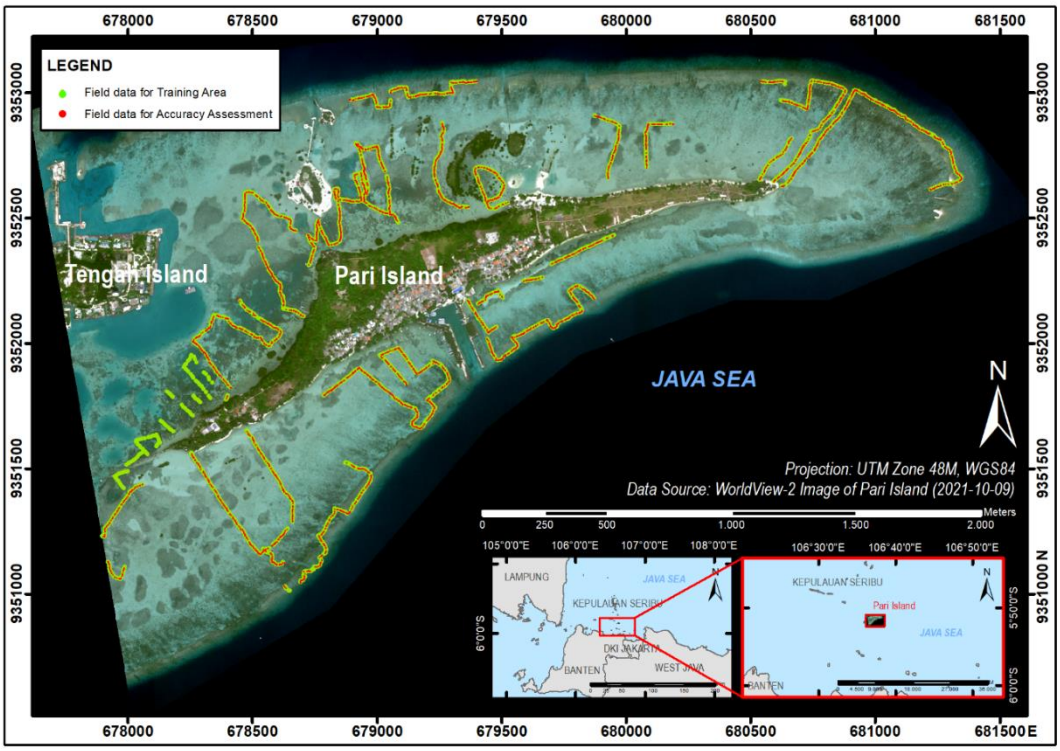

Figure 1. Map of study area and the distribution of field seagrass data

METHODS

Field Survey

Field surveys were conducted from February 26 to March 3, 2023, to collect data on the benthic cover of seagrass ecosystems and determine the percentage of seagrass cover at the study site. We utilized a conversion formula developed by Wicaksono et al. (2021a) to calculate the AGC based on the percent cover. During the field surveys, we employed the photo-transect technique (Roelfsema & Phinn, 2010). The transects were divided into two sets: one set was used to train the classification and regression algorithm, while the other set was used to assess the accuracy of the mapping results. To analyze the data from the photo-transect surveys, we used CPCe software (Kohler & Gill, 2006). The CPCe analysis output produced information on the percentage cover of benthic habitat and seagrass species. We then rasterized the resulting data based on the GSD of the WorldView-2 image (2 m). In cases where a single pixel of the WorldView-2 image contained multiple sets of CPCe data, we calculated the average value for that pixel.

Image Corection

The WorldView-2 (WV2) ORStandard2A image product was acquired on October 9, 2021, and received as radiometrically calibrated digital numbers (DN). The specifications of the WV2 used in this study are provided in Table 1. The conversion from DN to Top-of-Atmosphere (TOA) spectral radiance and reflectance followed the procedure described in Updike & Comp (2010). Initially, the FLAASH method was chosen for atmospheric correction. However, the aerosol optical depth (AOD) at 550 nm product from MODIS (Bhatia et al., 2018), which is required to estimate the visibility value for FLAASH input, was not available on the date when the WV2 image were acquired. Consequently, the Dark Object Subtraction (DOS) method was employed to perform atmospheric correction on the WV2 images and to obtain surface reflectance (SR) bands from TOA reflectance bands. To determine the path radiance offset, the reflectance of clear optically deep water pixels was utilized as the reference samples. Since there was no presence of sunglint in the scene, sunglint correction was not applied. Additionally, water column correction was not necessary for our study due to the shallow reef flat nature of the seagrass meadows and minimal underwater topographic variations. Previous studies by Zhang et al. (2013) and Wicaksono et al. (2021b; 2022a; 2022b) have also emphasized the negligible impact of water column energy attenuation on this benthic habitat condition.

For the mapping activities, only optically shallow water areas were considered, and land and optically deep water pixels were excluded. Land pixels were masked out based on the thresholding of the NIR band, while unsupervised ISODATA classification was performed to identify the cluster of optically deep water areas, and the corresponding pixels of that cluster were removed.

Table 1. WorldView-2 image specifications used in this study

Acquisition date	October 9, 2021
Ground Sampling Distance (GSD) (m)	2
Dynamic range	11-bits per pixel
Spectral bands	Wavelength (nm)
• Coastal	400 - 450
• Blue	450 - 510
• Green	510 - 580
• Yellow	585 - 625
• Red	630 - 690
• Red Edge	705 - 745
• Near Infrared (NIR) 1	770 - 895
• Near Infrared (NIR) 2	860 - 1040
Off-nadir viewing	21.6°

WorldView-2 Derivatives

Several image transformations were applied to the WV2 SR bands in order to obtain derivative data that could enrich the mapping input during the mapping process. These transformations were selected based on their successful application in previous works focusing on benthic habitat and seagrass mapping, including Principle Component Analysis (PCA), co-occurrence texture analysis, and band ratios (Wicaksono, 2016; Wicaksono, et al., 2022a; Wicaksono et al., 2022b; Wicaksono et al., 2022c). For PCA, all six bands ranging from coastal to red-edge bands were used as input, and the resulting PC bands were subset up to 99% of the total eigenvalues, which translates to the first three PC bands. PC4 to PC6 were considered as noise based on eigenvalue statistics and visual assessment of the resulting image. The co-occurrence texture analysis utilized mean and variance variables. Specifically, there are six mean texture bands and six variance texture bands, each derived from the visible bands. Additionally, 15 band ratios were obtained by calculating the ratios between visible bands. In total, these derivative data, combined with the SR bands of WV2, amounted to a total of 38 bands for the mapping process input.

Benthic Habitat Mapping

Benthic habitat mapping was primarily conducted to obtain the spatial distribution of seagrass and its substrate, enabling further analysis of percent cover and above-ground carbon stock (AGC) mapping. The following rules were applied: Dominated (i.e., Sg dominated, C dominated). If there is benthic type >80%, or <80% but other benthic types <20%. Addition (i.e., Sg + BS). If the differences between benthic types is >20%. Mixture (i.e., Mix Sg Bs). If the difference between benthic types is <20%.

The benthic habitat mapping classification scheme, based on these rules, resulted in 21 distinct classes. However, this led to an imbalanced distribution of training areas and accuracy assessment samples across the classes. Additionally, during our experiments with the 21 classes for benthic habitat mapping, we observed that the accuracy of mixed composition classes tended to be very low and susceptible to misclassification into other classes with similar compositions or to the more dominant benthic classes. For example, mixed seagrass and sand were often misclassified as seagrass with sand or the seagrass-dominated class. Therefore, we reduced the number of classes by generalizing the classes based on the similarities in class composition and the misclassification rate between classes. As a result, we identified six different classes: Coral dominated (C dominated), Bare substrate dominated (BS dominated), Macroalgae dominated (M dominated), Seagrass dominated (Sg dominated), Bare substrate with seagrass (BS + Sg), and Mixed classes (Mix BS C M).

The field data reclassified to the aforementioned six benthic habitat classes were used to train the RF algorithm. The number of trees (ntree) tested were 100, 200, and 300, while the function to determine randomly selected features employed the square root of all features instead of the logarithm to maximize the number of features involved in each iteration. The impurity function was set to the Gini coefficient.

Seagrass Percent Cover and Aboveground Carbon Mapping

Seagrass percent cover for each species was converted into aboveground carbon (AGC) values using the species-specific percent cover (PC) to AGC conversion formula developed by Wicaksono et al. (2021a). For species such as Cs and Tc, which did not have a species-specific formula, a common PC to AGC conversion formula described in Wicaksono et al. (2021a) was applied. The total AGC for each plot sample was calculated as the sum of the AGC values for all species within the plot. Subsequently, the field PC and AGC data were utilized as training areas for RF regression algorithm to model seagrass PC and AGC using various derivative WorldView-2 bands

as inputs. The ntree tested were 100, 200, and 300, and the square root of all features was used to determine randomly selected features.

Accuracy Assessment

The accuracy of the benthic habitat mapping results was evaluated using a confusion matrix, which yielded values for overall accuracy (OA), user's accuracy (UA), and producer's accuracy (PA) (Congalton & Green, 2019). The mapping of PC and AGC utilized the root mean square error (RMSE) and plot 1:1 between predicted and reference PC and AGC values. Field data that were not used to train the RF classification and regression models were employed for the accuracy assessment, ensuring unbiased evaluation of the results. The research flowchart is provided in Figure 2.

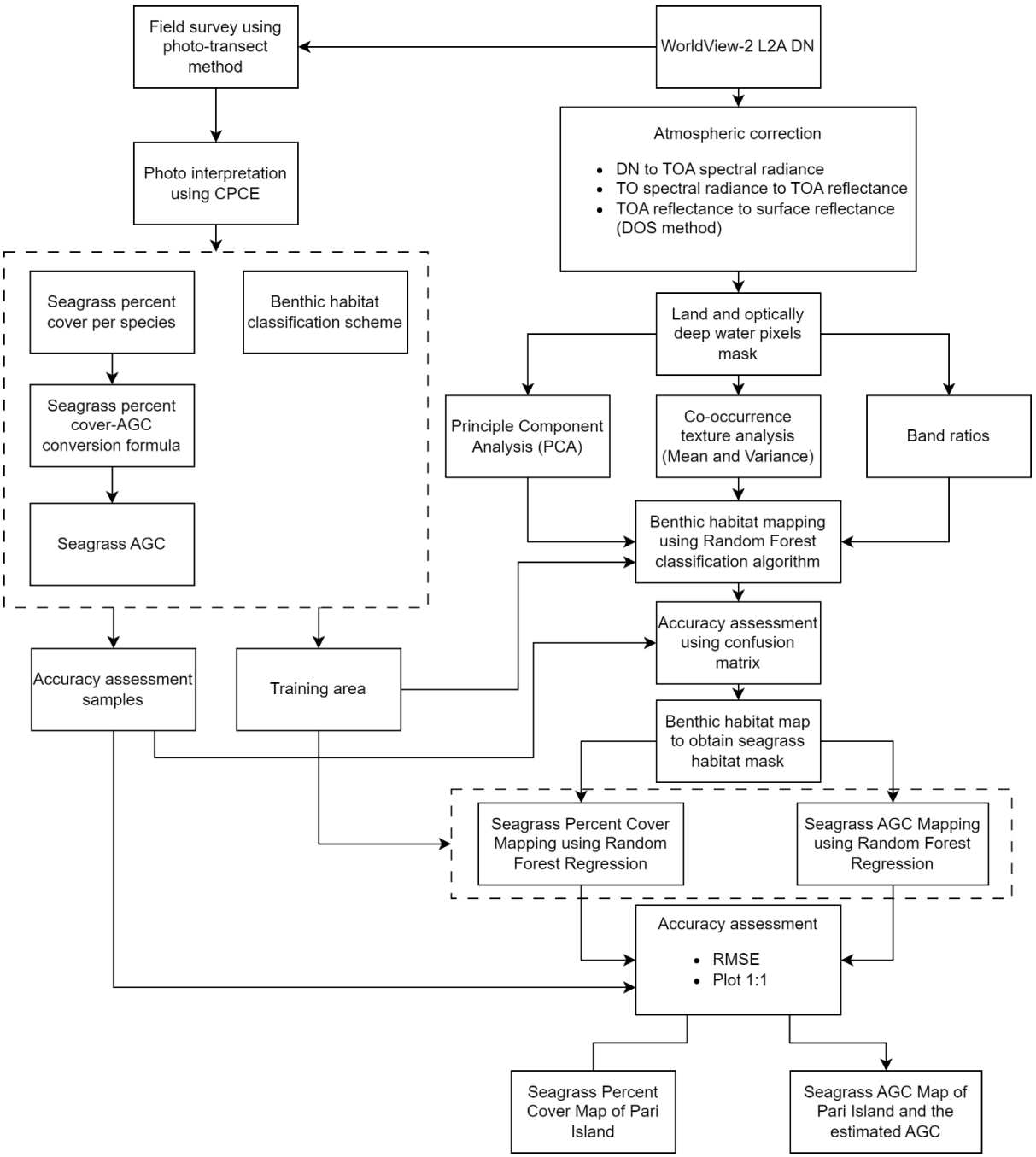

Figure 2. Research flowchart of mapping seagrass biodiversity indicators of Pari Island using multiple Worldview-2 bands derivatives

RESULTS

Field Seagrass Data

The summary of field data for benthic habitat, seagrass PC, and seagrass AGC mapping is provided in Table 2. The distribution of data for training area and accuracy assessment are covering similar range and comparable.

Table 2. Summary of field seagrass data collected in the field. All data have been standardized to 2 m GSD of WV2 image.

Benthic habitat classes		
Class	**Training area**	**Accuracy Assessment**
BS + Sg	402	403
Bs dominated	869	869
C dominated	1047	1047
M dominated	88	90
Mix BS C M	167	168
Sg dominated	1214	1105
Total	3787	3682
Seagrass PC	**Training area**	**Accuracy Assessment**
Min (%)	0	0
Max (%)	100	100
Average (%)	52	51.8
Std deviation (%)	20.3	20.6
Total	1508	1516
Seagrass AGC	**Training area**	**Accuracy Assessment**
Min (g C m^{-2})	3.7	3.7
Max (g C m^{-2})	35.5	35.5
Average (g C m^{-2})	12.9	12.9
Std deviation (g C m^{-2})	6.9	6.9
Total	1508	1516

Benthic Habitat Mapping

The most accurate benthic habitat map was obtained from combined input bands using ntree 200 with 65.2%. However, the accuracy difference between using 100, 200, and 300 ntree is very small with 0.2% (Table 3). Compared to other input, the accuracy difference range between 2.2% (with SR bands) to 10.7% (with PC bands). Table 2 also indicate that using more input bands deliver better benthic habitat mapping accuracy where combined inputs delivered the highest accuracy on all ntree scenarios. However, derivative bands of WV2 reflectance not necessarily give improvement to the mapping effort compared to the initial SR bands. In fact, SR bands produced the second best accuracy after the combined inputs and derivative information such as from band ratios, texture bands, and PC bands produced lower mapping accuracy. Furthermore, it is also evident that increasing ntree above 100 does not have any effect on the mapping accuracy and in our case the highest mapping accuracy came from ntree 200 in all inputs except SR bands. Nevertheless, the difference of accuracy between ntree is 1-2% only.

Table 3. Summary of accuracy assessment of benthic habitat mapping using various inputs

Input	n_{tree}		
	100	200	300
SR bands	62.6	62.6	63.0
Band Ratio	54.6	55.6	54.8
Texture bands	61.9	62.5	62.4
PC bands	53.9	54.5	54.1
Combined inputs	65.0	65.2	65.0

Figure 3 shows the spatial distribution of benthic habitat in the Pari Island based on the most accurate benthic habitat map (65.2%, combined inputs, ntree 200). The confusion matrix is provided in Table 4. Specifically for seagrass class (Sg dominated), the UA and PA are 65.2% and 72.8%, respectively. The majority of misclassification of seagrass class are with BS + Sg, BS dominated, and C dominated. While the misclassification between seagrass and BS + Sg and BS dominated class can be addressed by the inclusion of seagrass of varying density in their class descriptor, the misclassification with C dominated class mainly due to the water turbidity issue. The misclassification between seagrass and C dominated mainly occurring in the water in reef flat and lagoon in the north western part of Pari Island (red polygon in Figure 3). This area is dominated by Ea species covered by epiphytes living in a soft substrate and relatively turbid water, hence the seagrass reflectance is darker, and thus, the reflectance of seagrass in this area become similar to the coral reef in deeper water such as in fore reef area and misclassified to C dominated. Meanwhile, the reef crest and fore reef area and deeper lagoon are correctly dominated by C dominated class despite some pixels also classified as seagrass (blue polygon in Figure 3). Despite some areas of seagrass in the northwestern being misclassified as C dominated class, the distribution of seagrass is still overestimated due to the pixels in the reef crest and fore reef being misclassified as seagrass. Pixel classified as Sg dominated, BS + Sg, and BS dominated were further used to perform seagrass PC and AGC mapping.

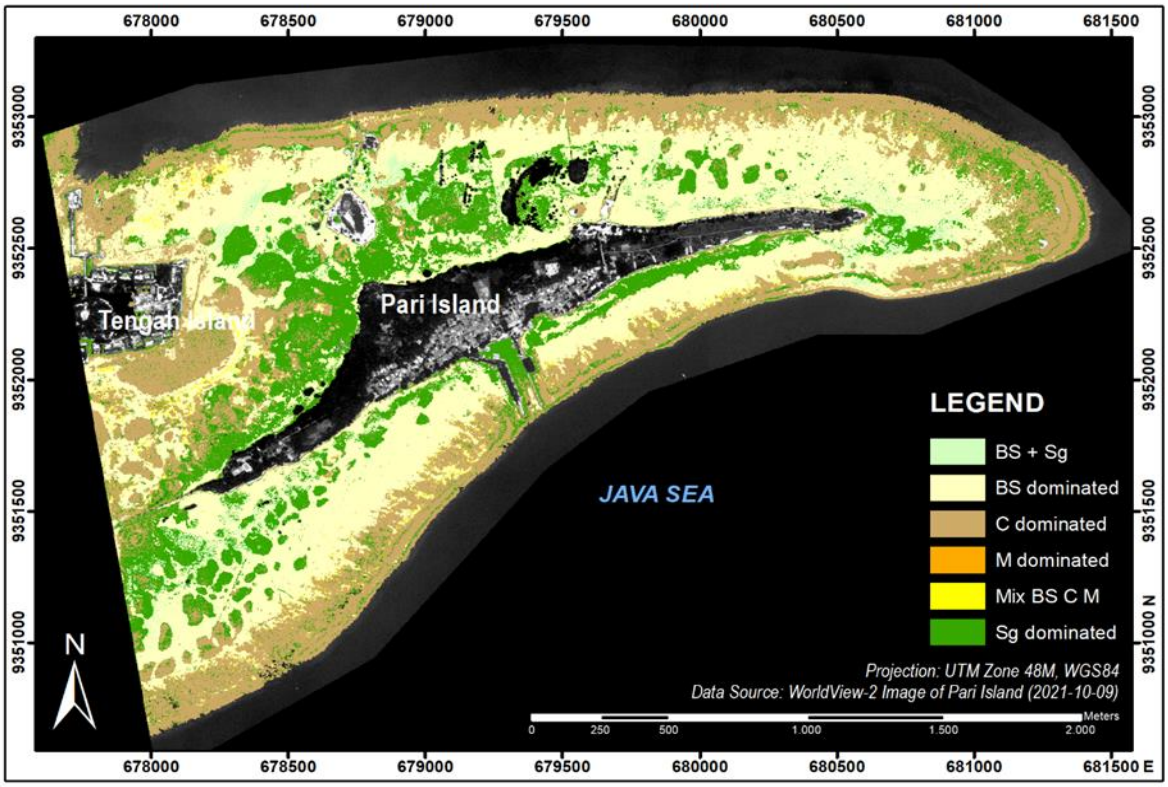

Figure 3. Benthic habitat classification using RF algorithm with ntree 200 using combined input (OA 65.2%). Red polygon shows the location where seagrass was misclassified as coral. Blue polygon shows the location where coral was misclassified as seagrass.

Table 4. Confusion matrix for the accuracy assessment of benthic habitat mapping

Map class	Reference						Total	UA (%)
	BS + Sg	BS dominated	C dominated	M dominated	Mix BS C M	Sg dominated		
BS + Sg	56	39	3	0	2	43	143	39.2
BS dominated	136	654	42	16	73	124	1045	62.6
C dominated	16	52	854	62	75	126	1185	72.1
M dominated	0	2	0	1	1	2	6	16.7
Mix BS C M	5	13	5	4	12	4	43	27.9
Sg dominated	186	107	122	7	5	803	1230	65.3
Total	399	867	1026	90	168	1102		
PA (%)	14.0	75.4	83.2	1.1	7.1	72.9	**OA = 65.2%**	

Seagrass PC Mapping

Similarly to benthic habitat mapping results, the most accurate seagrass PC mapping was produced from combined input using either 100, 200, or 300 n_{tree}. The most accurate RMSE is 17.1%. Nevertheless, the difference between the lowest and highest RMSE between inputs and n_{tree} is only 1.2%. Again, there is no substantial benefit in improving n_{tree} beyond 100 in the seagrass PC mapping accuracy in all inputs (Table 5). In comparison to benthic habitat mapping, the variation in accuracy in seagrass PC mapping is negligible between inputs and n_{tree} scenarios.

Table 5. Summary of accuracy assessment of seagrass PC mapping using various inputs

Input	n_{tree}					
	100		200		300	
	R^2	RMSE (%)	R^2	RMSE (%)	R^2	RMSE (%)
SR bands	0.28	17.5	0.28	17.5	0.29	17.4
Band Ratio	0.21	18.3	0.21	18.3	0.21	18.3
Texture bands	0.31	17.3	0.31	17.3	0.31	17.2
PC bands	0.22	18.2	0.22	18.2	0.23	18.1
Combined inputs	0.32	17.1	0.32	17.1	0.32	17.1

Figure 4 shows that the seagrass PC distribution is overestimated on lower percent cover. For instance, in pixels classified as BS dominated, the percent cover was predicted as 20 – 40%. The higher seagrass PC mainly located near the shoreline with the highest predicted seagrass PC are located in the northern side of Pari Island, mainly consist of Ea species covered by epiphytes. The predicted seagrass PC values range from 14.9% to 88.4% with the average of 47.4 ± 9.9%. Meanwhile, the reference seagrass PC values range from 0% to 100% with the average of 51.8 ± 20.6%. Although the average difference between predicted and reference seagrass PC is only 4.4%, due to the much lower standard deviation value, the predicted seagrass PC did not comprehensively captured the variation of seagrass PC in the study area, especially in the very low and very high seagrass PC. The very low seagrass PC was overestimated and the very high seagrass PC was underestimated.

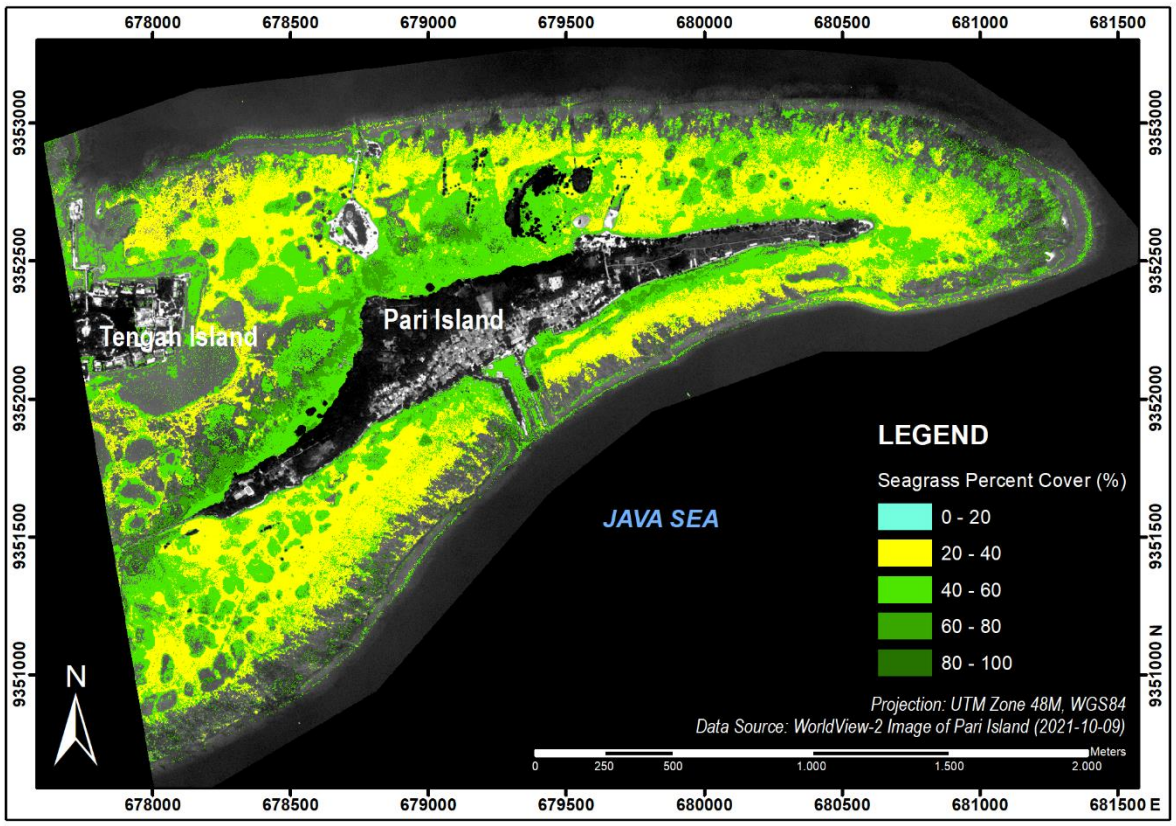

Figure 4. Seagrass PC map with 17.1% RMSE derived from combined inputs and RF regression with 100 ntree

Seagrass AGC Mapping

The results of seagrass AGC mapping is consistent between input and n_{tree} scenario (Table 6). The most accurate map obtained from combined input with RMSE 5.0 g C m^{-2}, but the RMSE difference between the most and least accurate result is only 0.6 g C m^{-2}. The R^2 between predicted and reference AGC is higher than those of seagrass PC. Furthermore, the difference between predicted and reference AGC is smaller than those in seagrass PC. The predicted AGC values range between 6.2 – 29.1 g C m^{-2} with average of 12.4 ± 4.1 g C m^{-2}. In comparison, the reference AGC range between 3.7 – 35.5 g C m^{-2} and average of 12.9 ± 6.9 g C m^{-2}. This is potentially because the reference seagrass AGC value per sample site to train the RF model and assess the accuracy of the resulting map is obtained from the AGC value from each species. This species-specific unique AGC values in return provide better variation when used to train the RF model. Furthermore, the seagrass AGC which is related to its biomass and LAI also a better proxy for the interaction of downwelling irradiance and the seagrass reflecting tissue in comparison to PC.

Table 6. Summary of accuracy assessment of seagrass AGC mapping using various inputs

Input	n_{tree}					
	100		200		300	
	R^2	RMSE (g C m^{-2})	R^2	RMSE (g C m^{-2})	R^2	RMSE (g C m^{-2})
SR bands	0.43	5.2	0.44	5.2	0.44	**5.1**
Band Ratio	0.34	5.6	0.34	5.6	0.35	**5.5**
Texture bands	0.45	**5.1**	0.45	**5.1**	0.45	**5.1**
PC bands	0.36	**5.5**	0.36	**5.5**	0.36	**5.5**
Combined inputs	0.47	5.1	0.47	**5.0**	0.47	5.1

The seagrass AGC map still indicate an overestimation in pixels classified as BS dominated and high seagrass AGC was only situated in the northwestern part of the island dominated by Ea with epiphytes (Figure 5). The medium and high seagrass PC areas near the shoreline in other areas are having lower AGC than the Ea dominated beds due to their species composition mainly consist of smaller species such as Th and Cr. At similar PC value, bigger species such as Ea has higher AGC than the smaller species. This adds and provide better dynamics and variations in the predicted AGC values. In general, the map shows that lower seagrass AGC (mainly <10 g C m^{-2}) tends to be overestimated, while the higher seagrass AGC, mainly above 22 g C m^{-2}, tends to be underestimated (Figure 6). From the map, it is estimated that the study area store 27.9 ton C of seagrass aboveground biomass.

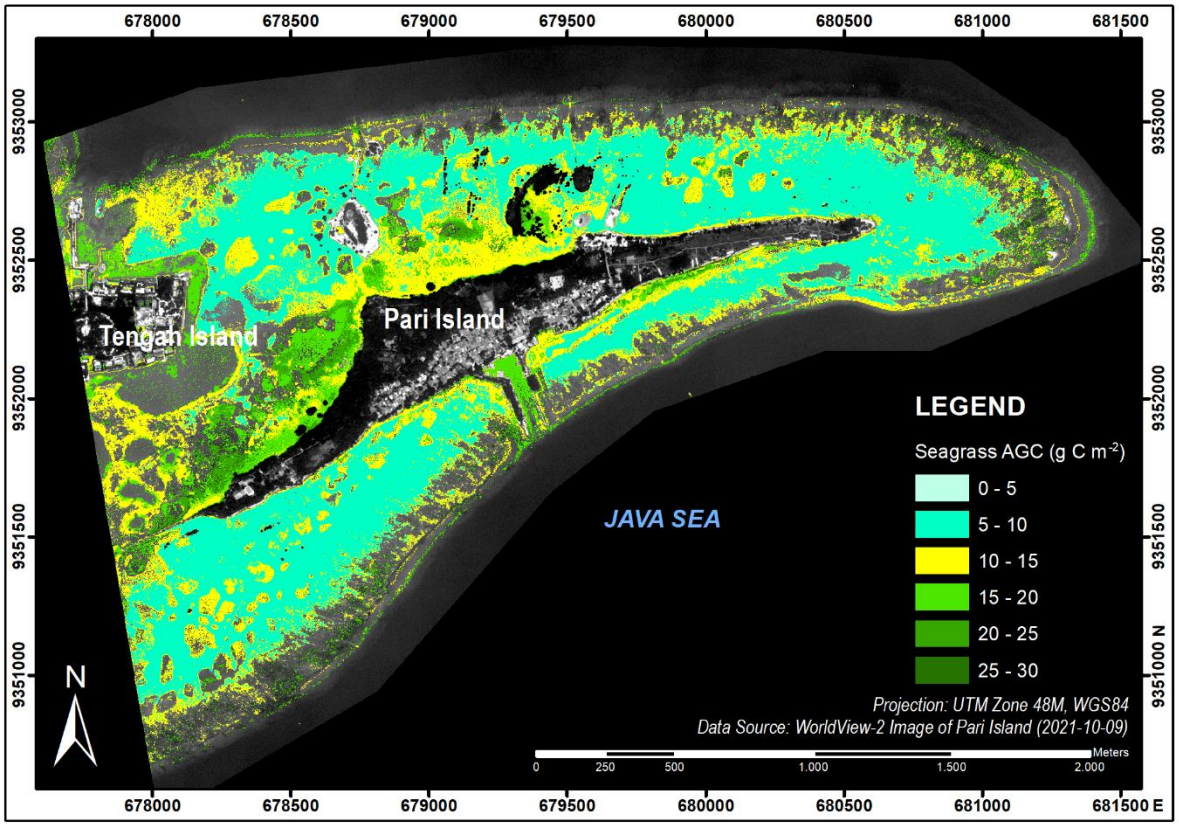

Figure 5. Seagrass AGC map with 5.0 g C m-2 RMSE derived from combined inputs and RF regression with 200 ntree.

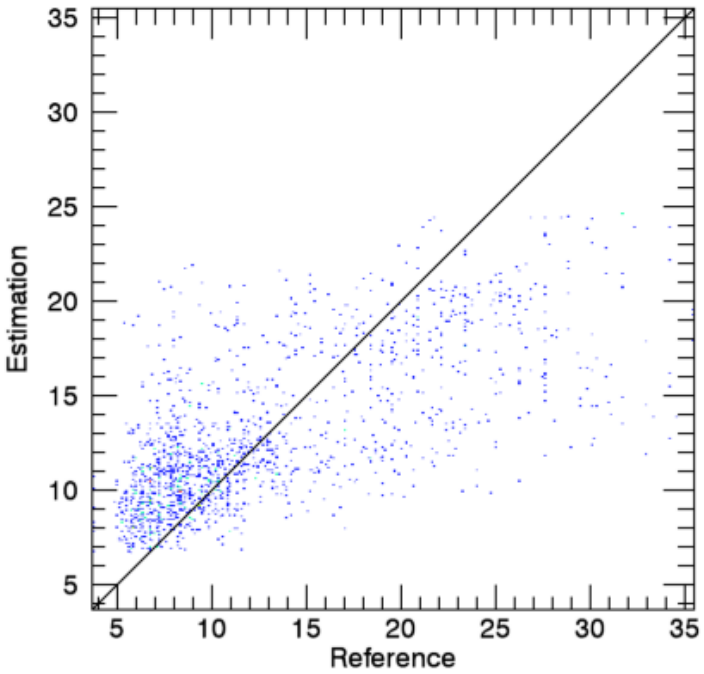

Figure 6. Scatter plot between reference and estimated seagrass AGC (g C m-2) from combined input with RMSE 5.0 g C m-2

DISCUSSION

Using high spatial resolution satellite imagery is generally expected to yield high accuracy. However, this expectation does not necessarily hold true for seagrass mapping. Seagrass mapping poses significant challenges in remote sensing due to various factors. These include water column energy attenuation, low signal-to-noise ratio (SNR) for water bodies, the mixing of benthic cover, similarity in reflectance across benthic cover, complex spatial structures, and the dynamic nature of seagrass meadows.

According to Wicaksono et al. (2022c), seagrasses exhibit monthly and seasonal growth patterns. This highlights that temporal resolution is as crucial as spatial, spectral, and radiometric resolution when it comes to mapping. Among the available multispectral satellite images in the market, WorldView-2, along with WorldView-3, stands out due to its high spectral and spatial resolutions. However, it is important to note that this option comes at a higher cost and faces challenges related to temporal resolution. Unlike resources such as PlanetScope, Sentinel-2, and Landsat, WorldView-2 lacks a consistent archive of time series data. This discrepancy in data availability between field data collection and image acquisition dates complicates the process of seagrass mapping.

The WV2 imagery used in this research was obtained on October 9, 2021, while the field survey was carried out from late February to early March 2023. Although this is not a big concern for coral reef mapping, it could lead to misclassifications in benthic habitat mapping, particularly for seagrass. It might also contribute to higher RMSE values in seagrass PC and AGC mapping. It is important to note that the seagrass PC observed in the field during February and March 2022 might not align with what the WV2 image captured in October 2021. This discrepancy is evident, especially for smaller species like Th and Cr, where the field-measured aboveground biomass could be either greater or lesser than what the WV2 image recorded.

Another consideration is the GPS geolocation accuracy, which is approximately ±3 meters. This accuracy limitation could potentially lead to a spatial mismatch between the real-world data and the corresponding pixel in the WV2 image. Additionally, factors such as water turbidity can affect the assessment of seagrass habitat. High water turbidity, resulting in darker reflectance, might create an impression of higher biomass than actually presents in the field. Conversely, areas with lower seagrass cover situated on bright carbonate sand might appear less dense in the WV2 image due to the dominant and reflective nature of the sand substrate. Furthermore, sub-pixel mixing of different benthic covers such as seagrass with macroalgae, sand with microbenthos, and areas with dead corals and rubble can alter the overall reflectance of seagrass as captured by the sensor. This indicates that several factors need to be carefully considered and adjusted for when interpreting seagrass-related data from the WV2 imagery.

As a result, having a higher resolution, such as WV2, does not always result in higher mapping accuracy. The accuracy of our benthic habitat mapping aligns with previous achievements, but our classification scheme involves more complex classes, describing benthic composition rather than just dominant benthic cover classes (Wicaksono & Lazuardi, 2018; Wicaksono & Lazuardi, 2019; Ginting et al., 2023). Regarding seagrass PC mapping, our work's RMSE is comparable to that of Fauzan et al. (2017) and Fauzan et al. (2021) using Sentinel-2. However, for seagrass AGC mapping, our RMSE is notably higher than the work by Wicaksono et al. (2022c) using Sentinel-2 in Labuan Bajo. Yet, it falls within the range of accuracy obtained by Wicaksono et al. (2022a) study using WorldView-2 on Parang Island. In addition to the aforementioned issues, these variations in accuracy and RMSE can be attributed to the differing characteristics of seagrass meadows. Wicaksono et al. (2022a) highlighted that mapping seagrass in patchy and continuous meadow conditions presents distinct challenges. Indeed, due to its higher GSD, WV2 delivers more precise maps that can effectively map seagrass at a finer scale compared to PlanetScope, Sentinel-2, or Landsat. The RMSE and misclassification of WV2 are calculated for a 2 × 2 m area, providing better precision for handling variations compared to the GSDs of 3 × 3 m, 10 × 10 m, and 30 × 30 m for PlanetScope, Sentinel-2, and Landsat, respectively.

Finally, our research has shown that a high spatial resolution image, represented by WV2 in this study, can effectively provide information about benthic habitat composition and maps of seagrass PC and AGC with a level of accuracy similar to that published in previous works. However, direct comparisons are limited due to variations in input data, mapping methods, and habitat complexity. Nonetheless, our findings serve as a reference to highlight that increasing image resolution does not always lead to improved mapping accuracy.

CONCLUSION

The objective of this research is to utilize the integration of WV2 derivatives, field seagrass data, and RF classification and regression algorithms to map seagrass distribution, PC, and AGC as a seagrass biodiversity indicator, in optically shallow water surrounding Pari Island. Our results show that the most accurate benthic habitat map has 65.2% OA with the UA and PA of Sg dominated class is 65.2% and 72.8%, respectively. The misclassification of seagrass mainly with C dominated (water turbidity issue), BS + Sg, and Mix Sg BS class (both contain seagrass in their class descriptor). The seagrass PC mapping yielded the most accurate RMSE of 17.1% and the average PC is 47.4 ± 9.9%. For the seagrass AGC mapping the most accurate RMSE is 5.0 g C m-2, with the average PC is 6.2 – 29.1 g C m-2 and the study area is estimated to store 27.9 ton C of seagrass aboveground biomass carbon stock. All the most accurate results for all these biodiversity indicators were produced from combined inputs, showing that more input bands delivered better accuracy when using RF algorithm. The addition of ntree beyond 100 also generally do not provide accuracy improvement. We also found that WV2 derivatives such as band ratios, co-occurrence texture bands, and PC bands did not improve the accuracy of SR bands when used individually. Thus, for seagrass mapping, it is encouraged to use combined bands from the derivatives of the

SR bands to maximize the information input to train the mapping algorithm instead of using the derivative bands individually or use the derivative bands as the replacement of the initial SR bands.

ACKNOWLEDGMENTS

This research is funded by the Faculty of Geography, Universitas Gadjah Mada, through the research grant scheme "Hibah Penelitian Mandiri Dosen Fakultas Geografi 2023."

DECLARATIONS

Conflict of Interest

The authors declared that they had no known competing interests.

Ethical Approval

On behalf of all authors, the corresponding author states that the paper satisfies Ethical Standards conditions, no human participants, or animals are involved in the research.

Informed Consent

On behalf of all authors, the corresponding author states that no human participants are involved in the research and, therefore, informed consent is not required by them.

DATA AVAILABILITY

Data used to support the findings of this study are available from the corresponding author upon request.

REFERENCES

Badan Pusat Statistik (BPS) Kepulauan Seribu. (2022). *Kabupaten Kepulauan Seribu dalam Angka 2022*. Jakarta: Badan Pusat Statistik (BPS) Kepulauan Seribu.

Bhatia, N., Tolpekin, V. A., Stein, A., & Reusen, I. (2018). Estimation of AOD Under uncertainty: an approach for hyperspectral airborne data. *Remote Sensing, 10*(947), 1-30. https://doi.org/10.3390/rs10060947.

Congalton, R. G., & Green, K. (2019). *Assessing the Accuracy of Remotely Sensed Data: Principles and Practices* (3rd ed.). Boca Raton: CRC Press, Taylor & Francis Group, LLC.

Fauzan, M.A., Kumara, I.S.W., Yigyantoro, R., Suwaedana, S., Fadhilah, N., Nurmalasari, I., Apriyani, S., & Wicaksono, P. (2017). Assessing the capability of Sentinel-2A data for mapping seagrass percent cover in Jerowaru, East Lombok. *Indonesian Journal of Geography, 49*(2). 195-203. Doi: http://dx.doi.org/10.22146/ijg.28407.

Fauzan, M.A., Wicaksono, M.A., & Hartono. (2021). Characterizing Derawan seagrass cover change with time-series Sentinel-2 images. *Regional Studies in Marine Science. 48*. 102048 Doi: https://doi.org/10.1016/j.rsma.2021.102048.

Fourqurean, J., Duarte, C., Kennedy, H. et al. (2012). Seagrass ecosystems as a globally significant carbon stock. *Nature Geosci.* 5. 505–509. https://doi.org/10.1038/ngeo1477.

Ginting, D.N.B., Wicaksono, P., & Farda, N.M. (2022). Mapping Benthic Habitat from WorldView-3 Image using Random Forest Case Study: Nusa Lembongan, Bali, Indonesia. In: *Int. Arch.*

Photogramm. Remote Sens. Spatial Inf. Sci. XLVIII-4/W6-2022. ISPRS. Johor Baru, Malaysia. 123-129.

Green E, Mumby P, Edwards A, Clark C. (2000). *Remote Sensing Handbook for Tropical Coastal Management*. Edwards, A.J., (Editor). Paris: The United Nations Educational, Scientific and Cultural Organization; 348 p.

Hochberg, E. J., Andrefouet, S., & Tyler, M. R. (2003). Sea surface correction of high spatial resolution ikonos images to improve bottom mapping in near-shore environments. *IEEE Transactions on Geoscience and Remote Sensing, 47*(1). https://doi.org/10.1109/TGRS.2003.815408.

Hossain, M.S., Bujang, J.S., Zakaria, M.H., & Hashim, M. (2015). The application of remote sensing to seagrass ecosystems: an overview and future research prospects. *International Journal of Remote Sensing, 36*(1). 61-113. https://doi.org/10.1080/01431161.2014.990649.

Kohler, K.E. & Gill, S.M. (2006). Coral Point Count with Excel extensions (CPCe): a Visual Basic program for the determination of coral and substrate coverage using random point count methodology. *Comput. Geosci.* 32 (9). 1259–1269. DOI: https://doi.org/10.1016/J.CAGEO.2005.11.009.

Mishra, D., Narumalani, S., Rundquist, D., & Lawson, M. (2006). Benthic habitat mapping in tropical marine environments using quickbird multispectral data. *Photogrammetric Engineering & Remote Sensing*. 72(9). 1037–1048.

Nordlund, L.M., Koch, E.W., Barbier, E.B., & Creed, J.C. (2016). Seagrass Ecosystem Servicesand Their Variability across Genera and Geographical Regions. *PLoS ONE. 11*(10): e0163091. https://doi.org/10.1371/journal.pone.0163091.

Phinn, S., Roelfsema, C., Dekker, A., Brando, V., Anstee, J.. (2008). Mapping seagrass species, cover and biomass in shallow waters: An assessment of satellite multi-spectral and airborne hyper-spectral imaging systems in Moreton Bay (Australia). *Remote Sens Environ. 112*(8). 3413–3425. https://doi.org/10.1016/j.rse.2007.09.017.

Pittman, S.J., Roelfsema, C., Say, C., Swanborn, D., Thapa, B., Jensen, K., Baez, S. (2021). *Outlining a methodological pathway to improve the global seagrass map*. The Pew Charitable Trusts.

Roelfsema, C. M., & Phinn, S. R. (2009). *A Manual for Conducting Georeferenced Photo Transects Surveys to Assess the Benthos of Coral Reef and Seagrass Habitats version 3.0. Brisbane*, Australia: Centre for Remote Sensing and Spatial Information Science, The University of Queensland.

Roelfsema, C., & Phinn, S. (2010). Integrating field data with high spatial resolution multispectral satellite imagery for calibration and validation of coral reef benthic community maps. *Journal of Applied Remote Sensing, 4*(1). https://doi.org/10.1117/1.3430107.

Roelfsema, C.M., Lyons, M., Kovacs, E.M., Maxwell, P., Saunders, M.I., Samper-Villarreal, J., & Phinn, S.R. (2014). Multi-temporal mapping of seagrass cover, species and biomass: A semi-automated object based image analysis approach. *Remote Sensing of Environment, 150*. 172–187. https://doi.org/10.1016/j.rse.2014.05.001.

United Nations Environment Programme (UNEP). (2020). *Out of the blue: The value of seagrasses to the environment and to people*. UNEP, Nairobi.

Updike, T., & Comp, C. (2010). *Radiometric Use of WorldView-2 Imagery*. Longmont, Colorado: DigitalGlobe®.

Wicaksono, P. & Hafizt, M. (2013). Mapping seagrass from space: addressing the complexity of seagrass LAI Mapping. *European Journal of Remote Sensing*, 46(1). 18-39. https://doi.org/10.5721/EuJRS20134602.

Wicaksono, P., & Lazuardi, W. (2018). Assessment of PlanetScope Images for Benthic Habitat and Seagrass Species Mapping in A Complex Optically Shallow Water Environment. *International Journal of Remote Sensing, 39*(17), 5739-5765. https://doi.org/10.1080/01431161.2018.1506951.

Wicaksono, P., & Lazuardi, W. (2019). Random forest classification scenarios for benthic habitat mapping using planetscope image. 2019 IEEE International Geoscience and Remote Sensing Symposium (8245-8248). Yokohama: IEEE IGARSS 2019. https://doi.org/10.1109/IGARSS.2019.8899825.

Wicaksono, P. (2016). Improving the accuracy of multispectral-based benthic habitats mapping using image rotations: the application of principle component analysis and independent component analysis. *European Journal of Remote Sensing,* 49(1). 433-463. https://doi.org/10.5721/EuJRS20164924.

Wicaksono, P., Danoedoro, P., Hartono, Nehren, U., Maishella, A., Hafizt, M., Arjasakusuma, S., & Harahap, S.D. (2021a). Analysis of field seagrass percent cover and aboveground carbon stock data for non-destructive aboveground seagrass carbon stock mapping using WorldView-2 image. In: *Int. Arch. Photogramm. Remote Sens. Spatial Inf. Sci*, XLVI-4/W6–2021. ISPRS, Manila. 321–327.

Wicaksono, P., Fauzan, M. A., Kumara, I. S. W., Yogyantoro, R. N., Lazuardi, W., & Zhafarina, Z. (2019). Analysis of reflectance spectra of tropical seagrass species and their value for mapping using multispectral satellite images. *International Journal of Remote Sensing, 40*(23), 8955-8978. https://doi.org/10.1080/01431161.2019.1624866.

Wicaksono, P., Maishella, A., Arjasakusuma, S., Lazuardi, W. & Harahap, S.D. (2022a). Assessment of WorldView-2 images for aboveground seagrass carbon stock mapping in patchy and continuous seagrass meadows. *International Journal of Remote Sensing, 43*(8). 2915-2941. https://doi.org/10.1080/01431161.2022.2074809.

Wicaksono, P., Maishella, A., Lazuardi, W., & Muhammad, F.H. (2022b). Wicaksono, P., Maishella, A., Lazuardi, W., & Muhammad, F. H. (2022). Consistency assessment of multi-date PlanetScope imagery for seagrass percent cover mapping in different seagrass meadows. *Geocarto International, 37*(27), 15161-15186. https://doi.org/10.1080/10106049.2022.2096122.

Wicaksono, P., Maishella, A., Wahyudi, A.J., & Hafizt, M. (2022c). Multitemporal seagrass carbon assimilation and aboveground carbon stock mapping using Sentinel-2 in Labuan Bajo 2019–2020. *Remote Sensing Applications: Society and Environment*, 27. 100803. DOI: https://doi.org/10.1016/j.rsase.2022.100803.

Wicaksono, P., Wulandari, S.A., Lazuardi, W., & Munir, M. (2021b). Sentinel-2 images deliver possibilities for accurate and consistent multi-temporal benthic habitat maps in optically shallow water. *Remote Sensing Applications: Society and Environment, 23*. 100572. https://doi.org/10.1016/j.rsase.2021.100572.

Widisanto, H., Pranowo, W.S., Simanjuntak, S.M., & Setiadi, H. (2022). Studi konstanta harmonik pasang surut terhadap data suhu permukaan laut di perairan pulau pari: study of tidal harmonic constants on sea surface temperature data in pari island waters. *Jurnal Chart Datum. 2*(2).139-50. https://doi.org/10.37875/chartdatum.v2i2.100.

Zhang, C., Selch, D., Xie, Z., Roberts, C., Cooper, H., & Chen, G. (2013). Object-based Benthic Habitat Mapping in the Florida Keys from Hyperspectral Imagery. *Estuarine, Coastal and Shelf Science, 134*, 88-97. https://doi.org/10.1016/j.ecss.2013.09.018.